Project Title

A Dynamic Neural Architecture for Choice Reaching Tasks

Title of Target Journal

Neural Networks

Student Name

Ömer Bahadır Eryılmaz

Supervisor Name

Dietmar Heinke & Fan Zhang

Word Count

4944

Submitted in partial fulfilment of the requirements for the degree of Master of Science

School of Psychology

University of Birmingham

ACKNOWLEDGEMENT

Firstly, I would like to thank my supervisors, Dr Dietmar Heinke and Dr Fan Zhang for their patience, kindness, and help. I am grateful for having them as my supervisors.

Secondly, I want to thank all my friends I met in Birmingham, and special thanks to the friends who joined my study group. In a relatively short period of time, we built good friendships.

In regard to the dissertation, during the first semester we studied the dynamic field theory with Muhammed Maarufi and Nariman Emadzadeh. For all our group study sessions with Azka Ashraf, Ekrem Ekici, Mitchum Balley, Pei-Hsuan Lin, and others, their company was good, and all of our conversations were valuable, memorable, and fun. Considering the time we spent together, I may need to write a chapter just for Nariman, but I will finish with our motto: We will be fine.

Many thanks to all my friends from my hometown. Especially, I want to thank Ahmet Ulus, Cihan Katar and Mustafa Bayrak for their continuous support and friendship.

I would also like to express my sincere gratitude to the Turkish Ministry of the National Education (MoNE) for supporting my postgraduate education.

Of course, many thanks to my mother, sister, and my big family. They had a great role in every step of my achievements.

ABSTRACT

Recent research into choice reaching tasks (CRT) demonstrate that competition in visual attention before the decision is made can lead to a variety in reaching movements. This project aims to further develop an architecture to simulate Strauss and colleagues' (2015) robotic control mechanism, based on the findings from the CRT experiments. The presented model simulates the reaching experiments for odd-coloured targets (i.e. a red target among green distractors or vice versa) based on dynamic field theory (DFT) by using the COSIVINA framework to create DFT structures (Schöner et al., 2016). In accordance with the findings of CRT experiments, the model consists of two main stages which operate in parallel: the target selection stage and the motor stage. The spatially represented motor parameters and competition in the target selection allow the model to imitate the reaching trajectories from CRT experiments in a two-dimensional plane. Moreover, the model can also demonstrate the priming effect which means that reaching trajectories deviate less when the target colour is repeated in the following trials. Additionally, the model suggests that the reason behind the shorter initial latencies when the target colour is changed might be because of an initial high activation of the objects' representations. The results also demonstrate that symmetrically located distractors may reduce the deviations in the trajectories by cancelling each other out. Importantly, our study provides a novel graphical user interface (GUI) to lay the foundation for future studies. This GUI allows the user to change parameters while the model is running. Furthermore, modelling these experiments without a real robot is less costly and less time consuming.

1. Introduction

People have a limited capacity to process information, and the visual environment is highly complex for perceiving in-detail information at first glance. Selective visual attention is supposed to guide us in visual searches to deal with this complexity. According to the well-known models of this mechanism, "attention" emerges from the competition among objects in their neural representations (e.g., Desimone & Duncan, 1995; Heinke & Humphreys 2003). Many factors are involved in this competition, including the prior knowledge of the observer, context of the task at hand, colours, or sizes of objects, etc. Visual search experiments investigate these factors and their effects on object selection (Duncan, J., & Humphreys, 1989; Eckstein, 2011; Wolfe, J. M., & Horowitz, 2017). In a typical visual search experiment, observers are asked to confirm either the existence or the absence of a pre-determined object among the distractors in a visual scene (Wolfe, J. M, 1998). Observers are asked to press an allocated button or key on the keyboard when they find the object to indicate that they have seen it. This period between the presentation of the visual scene and pressing the button is called the reaction time which is an important indicator of the task difficulty. There are also experiments where the objective is to select the target which is different from the distractors by one feature, such as colour (e.g. Maljkovic & Nakayama, 1994). In these experiments, detecting the target is a more straightforward task than the visual search tasks. This is true regardless of the number of distractors. This is known as the pop-out effect. Moreover, repetition of the target feature in the following trials creates the priming of pop-out (POP) effect which makes the competition easier and reduces the reaction time (Maljkovic & Nakayama, 1994).

However, people not only detect objects, they also act towards them. Thus, analysing the visually guided actions may reveal the interaction between the visual attention and the motor system (Song & Nakayama, 2006). Song and colleagues conducted a series of choice

reaching task (CRT) experiments by asking the participants to reach the target as soon as they see it with their index finger instead of pressing any button (2006, 2008, 2009, 2013). They used three objects, one of which is the target and the other two are distractors with the same colour and the only difference between these two is their colour (e.g. red target and green non-targets or vice versa). In these trials, the initial latencies (IL), the movement time (MT) and the movement trajectories were recorded for each participant. Here, IL is the period between the beginning of the stimulus presentation and the movement. Deviations from the ideal trajectories are defined as the distance between the actual trajectory and an imaginary straight line drawn from the initial position of the hand to the target. Maximum deviation (MD) of the movement trajectory and IL are important parameters to evaluate the task difficulty (Song & Nakayama, 2006). A lower MD and a shorter IL indicate an easier task. The researchers showed that when the same target colour is used in all trials, MD and IL decrease (Song & Nakayama, 2006). This is seen as a POP effect for object selection. However, if the colours of the target and non-targets are randomly switched for each trial, this is not what happens. In this case, the researchers found that when the target colour is switched, IL gets shorter compared to the repetition tasks while the MD increases (Song & Nakayama, 2008). The effect of the target colour switch on the reaching trajectory may be an evidence of the parallel interaction between the visual attention and the motor system (Song & Nakayama, 2008).

Strauss and colleagues (2015) modelled Song and Nakayama's (2008) CRT experiments using a robotic arm instead of human participants. Their model utilized the dynamic field theory (Amari 1977; Schöner et al., 2016) and included two main stages which operate in parallel: target selection stage and motor stage. The present study aims to build an extended version of Strauss and colleagues' (2015) model in a computer simulation with a graphical user interface (GUI) rather than by using a real robot arm. To achieve this, we used COSIVINA framework written by Sebastian Schneegans (Schöner et al. 2016). COSIVINA is

an object-oriented framework that is used to create DFT elements in MATLAB. Thus, we modified some elements of COSIVINA and added new elements to meet the requirements of our model. This tool brings with it some advantages including, not needing a physical robot, being less costly, and also being less time-consuming. Furthermore, advantageous factors also include effective parameter tuning and explainability of the model which we will explain in the fourth section.

The next section will introduce the DFT framework and its elements. Then, how these elements were used in the model will be explained in the following section. After that, the GUI will be presented in a separate section. In the fifth section, we will describe the experiment and present our results. Finally, in the discussion section, our results, limitations of the model and future studies will be discussed.

2. Dynamic Field Theory

In our model, visual selection and movement executions are governed by the mathematical framework of the dynamic field theory (DFT). The DFT framework considers the activation patterns of neural populations in the brain (Erlhagen and Schöner, 2002; Schöner et al., 2016). Especially, the distribution of population activation (DPA) which is a specific neurophysiologic analysis method allows DFT framework to link its models with the experimental results. DPA transforms the firing rate of a neural population to a continuous distribution form over a feature space. However, DFT models work in a behavioural level and generally do not point us to a specific region of the brain. Instead, they may illustrate the activation patterns from the different regions or the combination of several DFT elements may illustrate a single activation region in the brain (see for some examples of DFT framework used in neurophysiological studies, Johnson, Simmering & Buss 2014; Wijeakumar & Spencer

2020). This framework is also used in robotic systems (e.g. Strauss et. al., 2015; Tekülve et.al., 2019).

The main characteristic of the theory is that the activations within the populations are controlled with an interaction kernel, which adjusts the strength of activation in the principle of local excitation and global inhibition. It means that while this interaction function strengthens the activation in a close region, it suppresses the noise effect and the distant activations from the other input sources. This feature makes DTF have stable states when presented with external stimuli. The dynamic changes in these responses create a control mechanism to model some cognitive abilities such as visual selection and action. We will now explain the DFT elements which were used in our model.

The basic functional element of DFT architectures is the dynamic neural field. The activation in the dynamic neural field, $u(x,t)$, evolves according to the following equation which was introduced by Amari (1977).

$$\tau \dot{u}(x,t) = -u(x,t) + S(x,t) + h + \int w(x-x')f[u(x',t)]\,dx' \quad (1)$$

$$output = \frac{1}{e^{-(bx)}} \quad (2)$$

In the equation (1), x determines a spatial coordinate which corresponds to a specific neuron in the field. Thus, each neuron in the layer can be tuned according to external inputs. If there are no external inputs, the neural activation remains stable at the negative resting level ($u(x,t) = h,\ h < 0$). Here, τ is the time scale and determines the system response time of the DFT element. Once the activation goes above the zero level, the sigmoid function (equation 2) generates an output value. In the sigmoid function the constant of b determines the steepness of the response.

Neural fields may consist of many neurons and dimensions or they may consist of only one neuron with zero-dimension as a single node. While the higher dimensional neural fields can process more features from the input such as the location and the colour of the object,

single nodes can be used as a switch for the purpose of selection. In this study, single nodes are used to detect the target colour. Here, the single node dynamics are determined by the following equation.

$$\tau \dot{u}(t) = -u(t) + S(t) + h + c\sigma(u(t)) + \xi(t) \quad (3)$$

These elements can be linked to each other via the lateral interactions. As mentioned before, the parameters of the interaction kernel, w(x), mainly shape the behaviour of DFT.

$$w(x) = w_{excite} \cdot \exp\left(\frac{-x^2}{2\sigma_w^2}\right) - w_{inhibit} \quad (4)$$

Here, w_{excite} determines the strength of the excitatory connections and σ defines the spread of this excitation. The last parameter, $w_{inhibit}$ shows the strength of global inhibition between neurons. The kernel makes the activation excitatory for close distances while maximising the activation for the neuron itself ($w(0) = w_{excite} - w_{inhibit}$) and makes the activation inhibitory for remote distances.

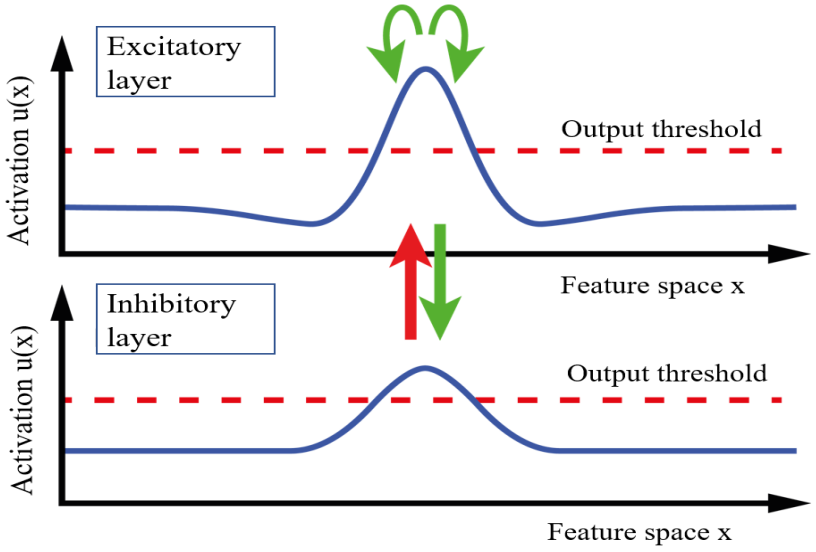

Fig.1. Two-layer field, modified from (Schöner et al., 2016). The green arrays (on top) demonstrate the self-excitation in the excitatory layer. The red array demonstrates the inhibitory connection from inhibitory layer to excitatory layer and the green array demonstrates the excitatory connection from excitatory layer to inhibitory layer.

Two-layer field is an extension of the dynamic neural fields. A typical two-layer field consists of excitatory and inhibitory layers which have the same feature space (**Fig.1**). The main feature of the two-layer field is that while the inhibition is conveyed by the inhibitory layer, the excitation is conveyed by the excitatory layer.

The two-layer field can model the behaviours of the neural populations such as transient waves (moving blob) and oscillations (Amari, 1977; Lu, Sato & Amari, 2011). In the current study, this element is used to create a moving blob by giving the visual information to the inhibitory layer. The changes of the blob location give a reference to obtain a proper velocity vector for each step (Strauss et al., 2015). It is important to note that this feature allows DFT to interface directly with visual perception and motor stages. This makes DFT eligible for the model to replicate Song and Nakayama's (2008) theory which states that there is a parallel interaction between motor movement and visual attention.

3. The Selection and Control Architecture

The current study is based on the previous work of Strauss et al., (2015), Choice reaching with a LEGO arm robot (CoRLEGO). The proposed model can simulate choice reaching tasks with an odd colour target based on Song and Nakayama's (2008) theory that says visual attention and motor system operate in parallel. In the model these mechanisms are represented in two main stages which operate simultaneously: the target selection stage and the motor stage.

3.1. The Target Selection Stage

The aim of this stage is to model the perceptual selection. For this reason, the stage includes red and green colour maps, a target colour map which consists of red and green colour nodes, and a target location map which is a dynamic neural field (see **Fig.2**) Before going into

the details of the process, it is useful to introduce these units. The colour maps are the matrices that keep the red and green colour channels of the target image. The target colour map provides the target colour information based on the competition between red and green nodes. The target location map represents the target location by receiving inputs from the colour maps and the target colour map.

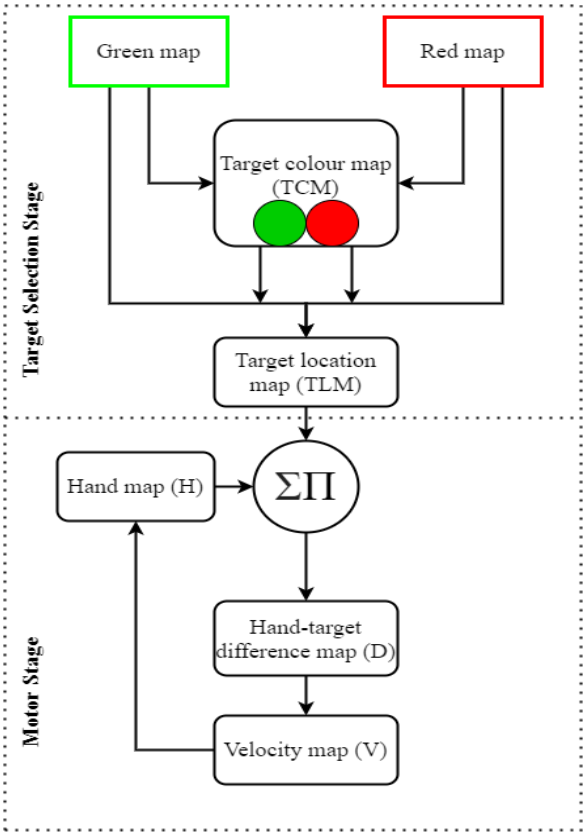

Fig.2. The model architecture. Modified from Strauss et al., (2015). The green and red maps are weighted by the outputs of the target colour map before proving the target location map an input. ∑ Π symbol represents convolution operation. The output of the velocity map controls the hand movement.

The process of the target selection starts once the input image is chosen. First, the target and distractor squares are represented in their own colour maps by being assigned from the red and green channels of the input image. After that the pixel summations of the red and green colour maps are multiplied by a coefficient, so that the summations are scaled to proper input values for the chosen parameters of the nodes (see **Appendix A**). These input values from the

red and green maps are fed into the green and red nodes, respectively. Here, there is a reverse feeding for colour nodes. The reason is that we want the node representing the target colour to win. Since all the parameters of these nodes are the same - and they are mutually, inhibitory connected- the competition is resolved in favour of the node which has the biggest input. Although during the competition both nodes can fire, at the end of the competition only the winner node will generate an output. In the following step, the matrix summation of the colour maps is weighted with the outputs of the target colour nodes. This weighted summation is the input of the target location map. Once the competition is over in the target location map, only the neurons representing the target location are activated and they suppress the other neurons along the field. However, competition in both maps happens simultaneously. This means that the neurons representing the target and distractors are both activated until the competition is over. This parallel process is consistent with Song and Nakayama's (2008) theory and it is important to model the curvature trajectories in the choice reaching tasks.

3.2. The Motor Stage

This stage aims to control the target-oriented movement in a continuous fashion by receiving input from the target location map (**Fig.2**). The knowledge of the target location is not enough by itself to generate such a movement. The model needs the knowledge of the target location relative to the hand position to produce the target-oriented movement. Therefore, the outputs of the target location map and the hand map are convolved to produce this information of the hand-target difference. The hand map includes a gaussian blob which represents the position of the hand. (It is important to note here that the negative values of the gaussian blob are capped to 0 because they create artifacts in the convolution. Also, the convolution result, namely, the hand-target difference is normalized and multiplied by a coefficient (see **Appendix A**). Adjusting this coefficient by using the slider in the GUI facilitates the parameter tuning

(**Fig.3**).) The blob in the hand map is initially located in the centre of the map then its position is updated according to a velocity vector.

Creating the velocity vector to provide a proper hand movement is the critical part of the motor stage. To generate such a vector the model utilises the two-layer DFT element (as mentioned in the section 2). The hand-target difference map (D) and the velocity map (V) are the excitatory and inhibitory layers of the two-layer field element, respectively (**Fig.1**). The names of the maps represent the functions of the layers. The hand-target difference map takes two inputs: the hand-target difference information and a fixed activation map which includes a gaussian blob located in the middle. Even if there are no external inputs for the velocity map, it can still demonstrate a "moving blob" behaviour via lateral interactions with the hand-target difference map (Amari, 1977; Strauss et al., 2015). During the competition process, the target location map may include more than one blob representing the target and distractors. These activation blobs at the corresponding locations impact the hand target difference map and distort the velocity vector until the end of the competition. If there are many activation blobs, the velocity vector heads towards the mean point of the activations (Lee et al., 1988). For this reason, the changes in the velocity vector causes variations in the movement trajectories. Once the velocity is obtained from the change in the activation blob's location, it is multiplied by α=0.01 to update the hand position in a proper way. Thus, when the distance between the hand and the target is zero, the gaussian blob in the hand-target difference map matches with the fixed gaussian blob in the centre and the hand movement stops.

4. The Graphical User Interface (GUI)

The main advantages of having a GUI include effective parameter tuning and visualisation. Parameter tuning is an important step in developing a model, because models need to have certain parameters to work properly. In the DFT framework, parameters are tuned

in accordance with the responses of the DFT elements since there is no specific algorithm to find the proper parameters (Lomp et al., 2016). Without a user interface the process of parameter tuning typically follows this order; set the parameters, run the code, observe the results then change the parameters, run the code again and repeat these steps until finding certain parameters to make a proper model. This can be highly time consuming and unmanageable considering that the complexity of the model is increased by adding new DFT elements and connections. Therefore, we built the GUI of our model by modifying some elements of the COSIVINA and adding new elements to this framework. In the parameter tuning, the GUI was extremely useful because it allowed us to change the parameters by using the sliders while observing the change in the activations simultaneously. In terms of parameter tuning the GUI provides more options besides the online slider control. It also allows us to add more precise parameters by using the parameter button. Once the proper parameters are obtained, they can be saved with the save button (the bottom right side of **Fig.3**).

The other advantage it provides is the visualisation. The GUI demonstrates the ongoing process in the maps. This makes it easier both detecting and fixing the problems when the model behaves unexpectedly. Moreover, observing the simultaneous activations gives us an understanding about how the parallel interactions between the target selection and motor stage work. Additionally, this increases the explainability of the model. For example, it provides us with an answer for how the model imitates the shorter initial latencies when the target colour is changed (see the explanation in *5.4 Results*).

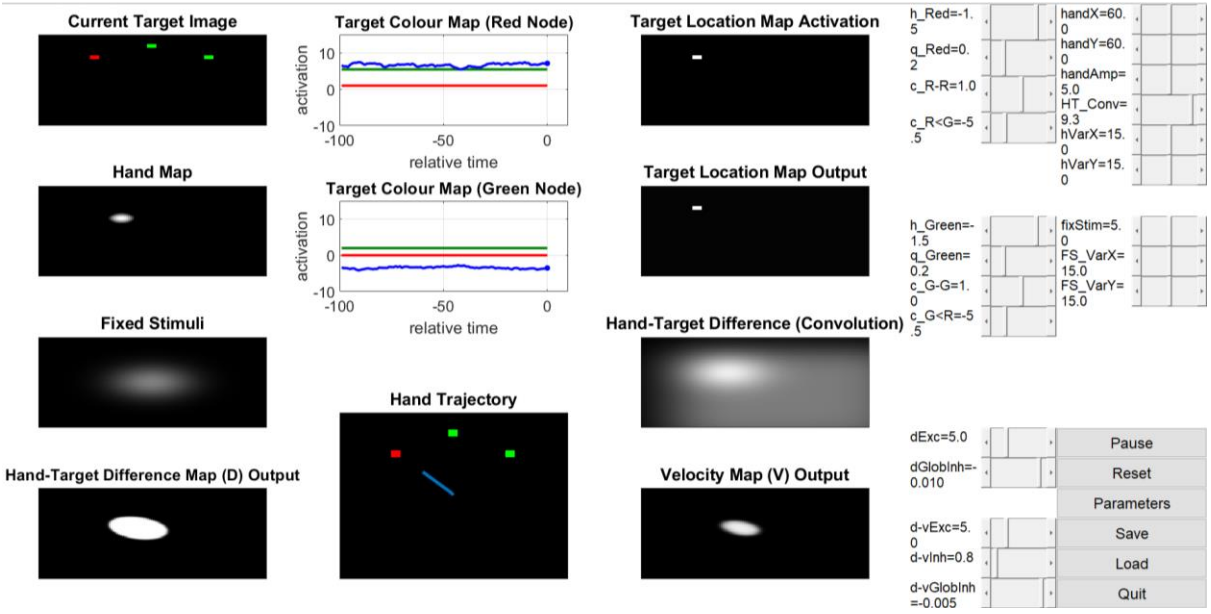

Fig.3. The graphical user interface (GUI) of the model. In the red and green nodes of the target colour map, blue, green, and red lines represent activation, input, and output, respectively. The gaussian blobs in the hand map and fixed stimuli have the same values (see the top right sliders in the **Fig.3** and **Appendix A**); however, only the apex of the hand blob is represented to make a better visualization for its movement. This movement is controlled by the velocity map (see *3.2. Motor stage* for the details).

5. Experiment

In the experiment, our aim was to simulate the odd-colour experiments by Song & Nakayama (2008). In order to do so, the model needed to replicate the effect of colour switching and repetition in the random-ordered trials. For the switched trials, initial latency (IL) was expected to be shorter; and maximum deviations of the trajectories and the movement time were expected to be higher than the repeated trials. This effect is known as the colour priming (Maljkovic & Nakayama 1994).

Unlike CoRLEGO, the pre-activation units were not needed in the current model for the colour priming. Since the trials were conducted with short breaks, the remaining neural activations from the previous trials provided this effect. Additionally, these activations also led to the positional (spatial) priming. Although the spatial priming was not reported by Song and

Nakayama (2008), it is reasonable to expect such an effect besides colour priming (Maljkovic & Nakayama, 1996; Strauss 2015). This effect will be discussed in the discussion section.

5.1 Methods

The hand movements were initiated when the peak activation in the velocity map moved from the centre and it passed the 0.5 threshold value. This threshold was added to prevent the noise of the velocity map from initiating the hand movement. Reaching trajectories were obtained from the hand movements. Maximum deviation (MD) for the trajectories was calculated by comparing the distances between each sample point on the trajectories and their correspondences on the straight lines which are the imaginary lines drawn from the starting point to the end point of the trajectory. Once the distance comparison of the point couples is done, the longest one was assigned as the MD of the trajectory.

The initial latency and the movement time were calculated from the velocity profile. The initial latency is the period between the beginning of stimuli and the initiation of the hand movement. However, in the model, the initial latency was defined as the period that starts with the presentation of the target image and ends with hand velocity passing over 0.04 (pixel/step) the first time. By doing this, we were able to compare our results with Song and Nakayama's (2008) findings.

5.1.1 Procedure

The input image of the target selection stage was chosen from the randomly ordered six combinations (**Fig.4**). Once this trial group was completed, another six combinations were randomly ordered. Then, this process was repeated 20 times for the total of 120 trials and each type of target image was chosen 20 times with different orders. Between each trial a black image was shown for 10 steps in simulation time.

For each trial, the hand movement was started from the centre of the input image. Additionally, 1250-time steps were given for each trial to complete the tasks and all tasks were completed in this period. The actual simulation time for all 120 trials was approximately 100 minutes.

5.1.2 Stimuli

The input images were 120 by 120 pixels and included three 5 by 5 square objects. The middle points of the square objects correspond to (30, 30), (60, 15) and (90, 30) pixel coordinates.

For each image, the odd colour object was the target and the other same colour objects were distractors. The red, green, and black colours used in the images had (0, 255, 0), (255, 0, 0), (0, 0, 0) RGB values.

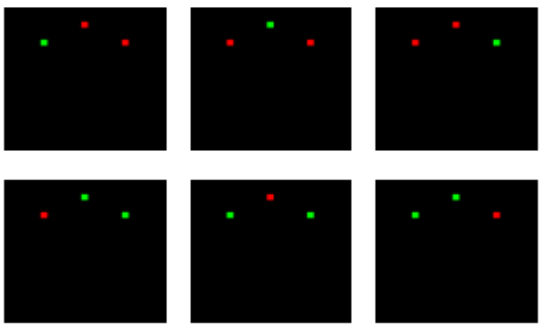

Fig.4. All target image combinations used in the trials. Green colour targets are on the top and red colour targets are on the bottom.

5.2 Results

The first requirement of a successful reaching movement is the selection of the correct target. Moreover, as we know from the CRT experiments, curve trajectories are mainly the result of the competition in this selection process (Song & Nakayama, 2006). Since the target

only differs from the distractors by its colour, securing a competitive and correct selection behaviour depends mostly on the target colour map, namely, the red and green nodes. Therefore, we tuned the self-excitation and mutual inhibition parameters, and the input of the nodes to create this behaviour. But even though the model had a competitive and correct selection behaviour, IL was not shorter for the switched trials. Then, we tuned the time scales, τ values, of the maps to imitate the shorter IL in Song and Nakayama's (2008) results. While smaller τ values made the maps response faster, bigger τ values had the opposite effect. Large response time differences between maps increased the curve of trajectories and caused the model to not reach the target. However, according to our parameter tuning experience, the response of target location map should be slower than the target colour map in order to secure the compatible IL (see parameters in **Appendix A**). This relatively slow response led to a memory effect in the target location map by keeping the correspondent neurons of the previous target location active for a while in the next trial. In addition, the colour switching initially activates the neurons which correspond to the distractors because their colour was the target colour of the previous trials. Thus, in our model we observed that switched trials had initially higher activations than repeated trials. These higher activations created stronger "pull effects" which caused higher rate accelerations of the hand velocity; hence they reduced the IL.

Once the parameters compatible for MD and IL values were tuned, the model was simulated in the experiment (see the results of the first 18 trials in **Fig.5**).

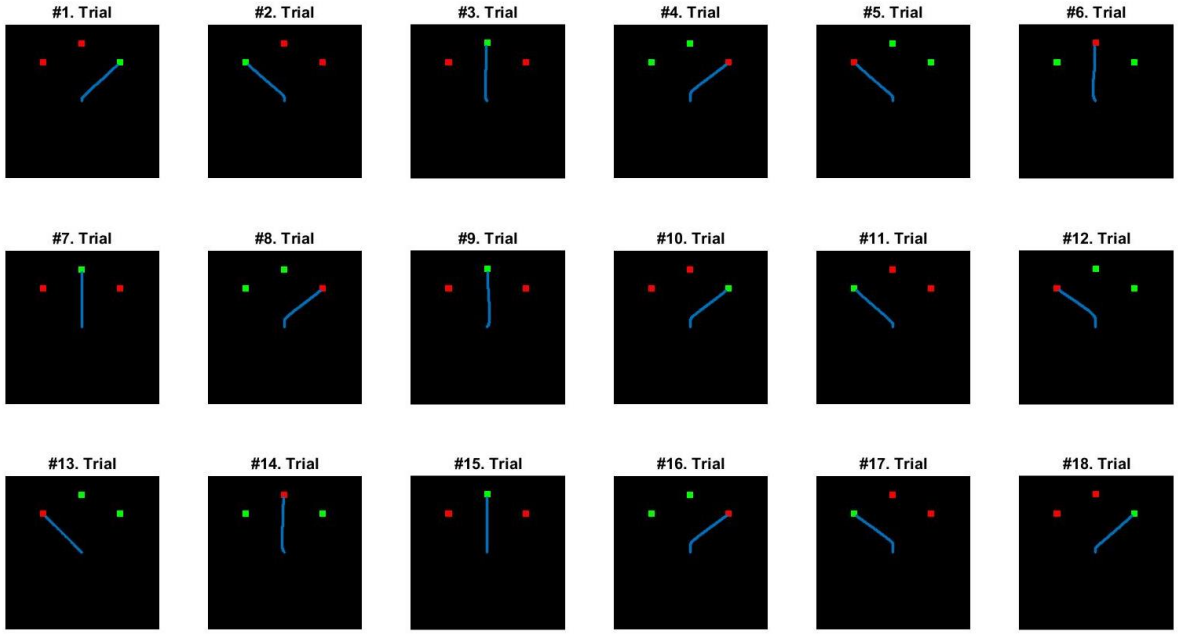

Fig.5. The hand-trajectories from the first eighteen trials are shown with the blue line. The hand moves from the centre of the images to the odd-coloured target. Trials with changed target colour show trajectories with more curvature; however, target position is also a factor in curve trajectories (see 6^{th}, 7^{th}, 11^{th}, 12^{th} and 14^{th}, 15^{th} trials).

To evaluate our results, we compared the maximum deviation (MD) of the reaching trajectories in trials with switched and repeated target colour. We also compared MD in trials when the target is in the middle and on the sides (**Fig.6**).

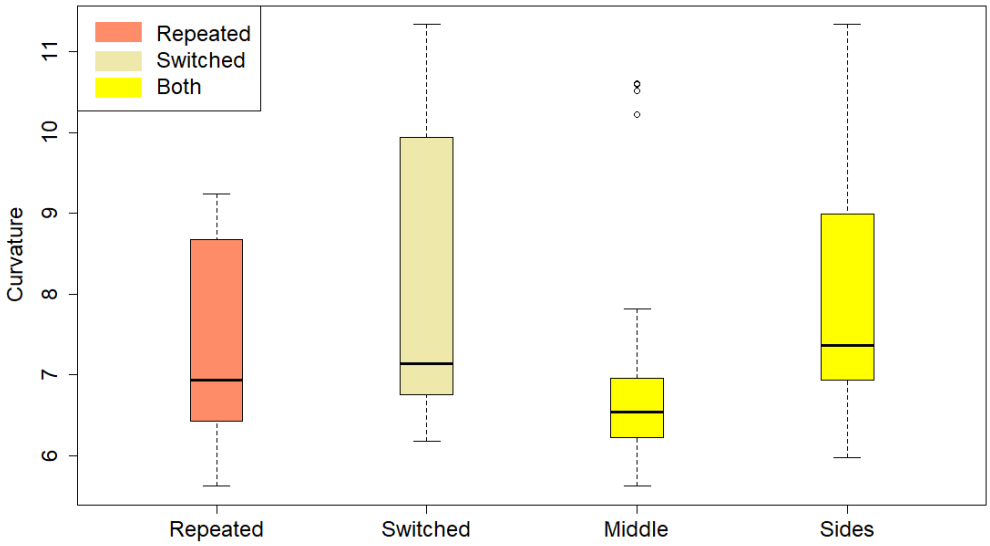

Fig.6. Maximum deviations (MD) of the reaching trajectories. It shows the trials with repeated and switched target colour and, the trials in which the target position was in the middle and on the sides. Interestingly, trajectories showed less curvature when the target was in the middle for both switched and repeated trials, except in 3 trials where the target colour and the position were changed.

Moreover, initial latency (IL), movement time (MT), and total time (TT) are compared in trials with switched and repeated target colour (**Fig.7** and **Table 1**). As expected, the movement time was longer for the switched trials since their trajectory lengths were longer than the ones in repeated trials. Additionally, although the average velocity profiles of both types of trials initially had different acceleration rates, their average velocities reached nearly the same peak level during the reaching movement (**Fig.8**).

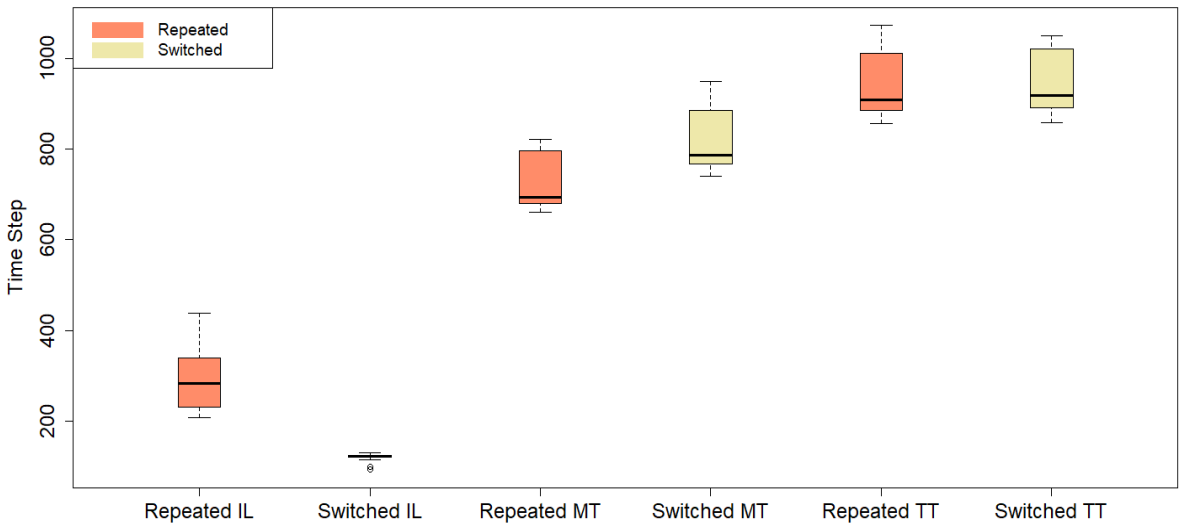

Fig.7. Initial latency (IL), movement time (MT), and total time (TT) of the trials with switched and repeated trials. The shorter initial latencies in switched trials compensate for the longer movement time and makes them as efficient as repeated trials in terms of total time.

Table 1

Welch Two Sample t-tests on the model's results. The tests illustrate that the model imitated the findings in CRT experiments of Song and Nakayama (2008). Trials with target colour switched had shorter initial latencies (IL) and longer movement time (MT). However, their total time (TT) was close to that of the target colour repeated trials. Moreover, maximum deviation (MD) was higher in colour switched tasks. Interestingly, MD changed significantly according to the target position (middle / sides).

Feature	N	Mean	t	Df	p-value
MD repeated	52	7.40	-2.08	116.07	<0.05
MD switched	67	7.92			
MD middle	40	6.95	-4.38	83.23	<0.001
MD sides	79	8.07			
IL repeated	52	294.65	21	52.29	<0.001
IL switched	67	120.25			
MT repeated	52	729.38	-7.71	113.34	<0.001
MT switched	67	815.33			
TT repeated	52	936.52	-0.97	109.82	= 0.33
TT switched	67	948.27			

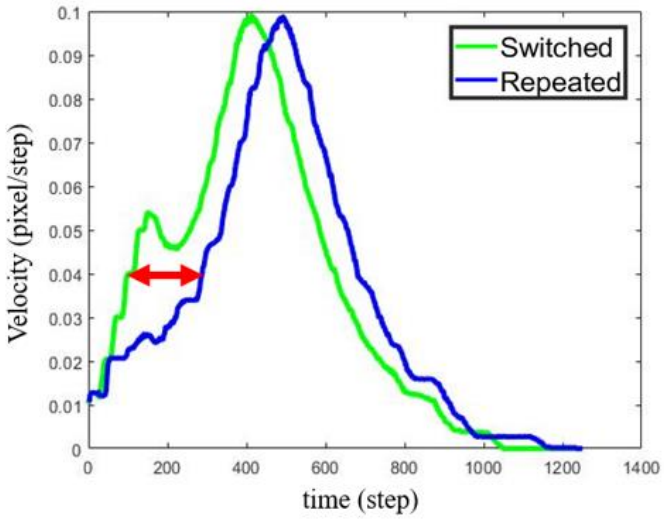

Fig.8. Averages of the hand velocities for the trials with switched and repeated target colour. The beginning of the movement time was determined as 0.04 velocity (pixel/step) and the red arrow points to the average time difference in the initial latencies between switched and repeated tasks.

5.Discussion

The main goal of the current study was to model Song and Nakayama's (2008) CRT experiments based on Strauss and colleagues' (2012, 2015) robotic control approach. The model was able to generate hand movements reaching towards the target in each trial (**Fig.5**). Moreover, trials with the switched target colour showed more curvature trajectories with shorter initial latency (IL) and longer movement time compared to the trials with the repeated target colour reported by Song and colleagues (2008, 2013) (**Table 1**).

Interestingly, our results also demonstrated that when the target was in the middle, the maximum deviations of the trajectories were smaller than the ones when the target was on the sides (**Fig.6** and **Table 1**). The reason for this result was the activations of neurons which represent the symmetrically located distractors. Because the spatial average of their activations corresponded to the direction of the target relative to initial hand position. This average effect of the activations is also the reason behind the curve reaching trajectories in our model.

Moreover, this average activation effect has also been demonstrated in neurophysiological studies. One of the first studies in this respect was done by Lee et.al. (1988). However, this result was not shown in the studies of Song and colleagues (2006, 2008, 2013). This is evidence for the spatial priming or any other distortion effect (noise) which can be more obvious in the lack of colour priming effect in human experiments.

The second aim of this study was to integrate the model with a specific GUI to facilitate the DFT model design (Lomp et. al.,2016) and to lay the foundations for the future studies. This GUI also illustrated that the initial higher activations of the target location map in switched trials allow the model to simulate shorter ILs in switched trials. Although this is the case in our model, there has not been any experiment supporting this conclusion. At the same time, Bastian, and colleagues' (2003) findings from their multi-directional pointing experiments with monkeys showed a strong correlation between IL and intense neural activation which points to the movement direction. In our model, initially higher activations include the representations of the distractors all of which point to the movement direction. Thus, future studies may compare ILs in human experiments using Song and colleagues' displays and the ones that include the same objects with closer distances. If they find shorter ILs in trials in which displays have closer objects, this may support our model's conclusions.

A limitation of this study is the 2-dimensional modelling of the CRT experiments. For a 3- dimensional simulation, one more layer can be added to the maps. The GUI is also adaptable to design this model and integrable with other simulation programs such as CoppeliaSim (Coppelia Robotics AG) for a better visualisation.

Future studies may simulate findings from the other CRT experiments (e.g. Moher & Song 2013, 2016) by adapting our model. These models provide an embedded visual and motor

mechanism for a very basic task. How this mechanism can deal with more complex tasks can be a question for the future studies.

References

Amari, S. I. (1977). Dynamics of pattern formation in lateral-inhibition type neural fields. Biological cybernetics, 27(2), 77-87.

Bastian, A., Schöner, G., & Riehle, A. (2003). Preshaping and continuous evolution of motor cortical representations during movement preparation. European Journal of Neuroscience, 18(7), 2047-2058.

Desimone, R., & Duncan, J. (1995). Neural mechanisms of selective visual attention. Annual review of neuroscience, 18(1), 193-222.

Duncan, J., & Humphreys, G. W. (1989). Visual search and stimulus similarity. Psychological review, 96(3), 433.

Eckstein, M. P. (2011). Visual search: A retrospective. Journal of vision, 11(5), 14-14.
Erlhagen, W., & Schöner, G. (2002). Dynamic field theory of movement preparation. Psychological review, 109(3), 545.

Heinke, D., & Humphreys, G. W. (2003). Attention, spatial representation, and visual neglect: simulating emergent attention and spatial memory in the selective attention for identification model (SAIM). Psychological review, 110(1), 29.

Johnson, J. S., Simmering, V. R., & Buss, A. T. (2014). Beyond slots and resources: Grounding cognitive concepts in neural dynamics. Attention, Perception, & Psychophysics, 76(6), 1630-1654.

Lee, C., Rohrer, W. H., & Sparks, D. L. (1988). Population coding of saccadic eye movements by neurons in the superior colliculus. Nature, 332(6162), 357-360.

Lomp, O., Richter, M., Zibner, S. K., & Schöner, G. (2016). Developing dynamic field theory architectures for embodied cognitive systems with cedar. Frontiers in neurorobotics, 10, 14.

Lu, Y., Sato, Y., & Amari, S. I. (2011). Traveling bumps and their collisions in a two-dimensional neural field. Neural Computation, 23(5), 1248-1260.

Maljkovic, V., & Nakayama, K. (1994). Priming of pop-out: I. Role of features. Memory & cognition, 22(6), 657-672.

Moher, J., & Song, J. H. (2013). Context-dependent sequential effects of target selection for action. Journal of Vision, 13(8), 10-10.

Moher, J., & Song, J. H. (2016). Target selection biases from recent experience transfer across effectors. Attention, Perception, & Psychophysics, 78(2), 415-426.

Schöner, G. (2016). Dynamic thinking: A primer on dynamic field theory. Oxford University Press.

Song, J. H., & Nakayama, K. (2006). Role of focal attention on latencies and trajectories of visually guided manual pointing. Journal of vision, 6(9), 11-11.

Song, J. H., & Nakayama, K. (2008). Target selection in visual search as revealed by movement trajectories. Vision research, 48(7), 853-861.

Song, J. H., & Nakayama, K. (2009). Hidden cognitive states revealed in choice reaching tasks. Trends in cognitive sciences, 13(8), 360-366.

Strauss, S., & Heinke, D. (2012). A robotics-based approach to modeling of choice reaching experiments on visual attention. Frontiers in psychology, 3, 105.

Strauss, S., Woodgate, P. J., Sami, S. A., & Heinke, D. (2015). Choice reaching with a LEGO arm robot (CoRLEGO): the motor system guides visual attention to movement-relevant information. Neural Networks, 72, 3-12.

Tekülve, J., & Schöner, G. (2019, August). Autonomously learning beliefs is facilitated by a neural dynamic network driving an intentional agent. In 2019 Joint IEEE 9th International Conference on Development and Learning and Epigenetic Robotics (ICDL-EpiRob) (pp. 143-150). IEEE.

Wijeakumar, S., & Spencer, J. (2020). A Dynamic Field Theory of visual working memory. Wolfe, J. M. (1998). What can 1 million trials tell us about visual search?. Psychological Science, 9(1), 33-39.

Wolfe, J. M., & Horowitz, T. S. (2017). Five factors that guide attention in visual search. Nature Human Behaviour, 1(3), 1-8.

Appendix A. Parameters

A.1. The parameters of the DFT elements

Map	τ	h	β	g_{inh}	c_{exc}	$\sigma_{exc(x,y)}$	c_{inh}	$\sigma_{inh(x,y)}$	c_q	$\sigma_{q(x,y)}$
TCM	10	-1.5	4	-	1	-	-5.5	-	0.2	-
TLM	20	-1	4	-	-	-	-	-	-	-
D	20	-5	4	-0.01	5	5	0	10	0.2	5
V	5	-0.2	4	-0.005	5	5	0.8	10	0.2	5

A.2. Other parameters

The hand map and the fixed stimuli are the same size matrices which include the same 2-dimensional gaussian blob (amplitude = 5, $\sigma_{x,y}$ =15).

The convolution of the hand map and the output of the target location map is multiplied by 9.3 after it is normalized.

Appendix B. Codes and Video Recording

B.1. Codes

The codes of the model can be found in the author's GitHub repository by using this link: https://github.com/OBEryilmaz/MScProject

B.2. Video Recording

The GUI of the model was recorded while the model is running. This video record can be found by using this YouTube link: https://www.youtube.com/watch?v=5GQnp0naEVc